

Switchable DNA-Based Peroxidases Controlled by a Chaotropic Ion**

Tanner G. Hoog,^{+, [a]} Matthew R. Pawlak,^{+, [a]} Lauren M. Aufdembrink,^[a] Benjamin R. Bachan,^[a] Matthew B. Galles,^[c] Nicholas B. Bense,^[d] Katarzyna P. Adamala,^[a, b] and Aaron E. Engelhart^{*[a, b]}

Here we demonstrate a switchable DNA electron-transfer catalyst, enabled by selective destabilization of secondary structure by the denaturant, perchlorate. The system is comprised of two strands, one of which can be selectively switched between a G-quadruplex and duplex or single-stranded conformations. In the G-quadruplex state, it binds hemin, enabling peroxidase activity. This switching ability arises

from our finding that perchlorate, a chaotropic Hofmeister ion, selectively destabilizes duplex over G-quadruplex DNA. By varying perchlorate concentration, we show that the DNA structure can be switched between states that do and do not catalyze electron-transfer catalysis. State switching can be achieved in three ways: thermally, by dilution, or by concentration.

Introduction

Biomolecules are highly attractive as potential programmable electron transfer catalysts and bioelectronics. A range of techniques have been employed, including microbial systems,^[1] protein-directed assembly of metal clusters,^[2] metallated base pairs,^[3] biopolymer-directed assembly of nanoparticles,^[4,5] and minimal peptides.^[6] With 0.34 nm spacing between nucleobases and exquisite, atomic-precision self-assembly directed by nucleobase hydrogen bonding, nucleic acids are an especially attractive means by which to develop programmable electron transfer catalysts. One means by which DNA can perform multiple turnover electron transfer is by employing a prosthetic group,^[7] as many enzymes that perform electron transfer in nature do.^[8] Hemin, one such prosthetic group, binds selectively to a noncanonical structure formed by G-rich sequences of

DNA, termed a G-quadruplex, which activates it to perform electron transfer.^[7,9,10] By binding hemin, the same prosthetic group employed by natural redox enzymes, such as peroxidases and cytochrome P450s, DNA can perform electron transfer in a biomimetic fashion while mitigating the oxidative damage issues associated with attempting to use it as a classical conductor.^[11]

Sequences of DNA and RNA that can exhibit either G-quadruplex or non-G-quadruplex (e.g., unpaired or Watson-Crick base paired) structures depending on context are a ubiquitous feature of life. These sequences are actively remodeled in living organisms.^[12-14] A bioinspired chemical system based on these phenomena that enabled reversible, programmable structure switching would afford a powerful tool for dynamic electron transfer behavior in DNA nanostructures. We thus sought to develop a chemical system to switch the same DNA between secondary structure states, reasoning that this would combine the speed and repeated reversibility of pH-switchable DNA nanomotors with the compatibility observed in static pH strand-exchange based systems.^[15-20]

Base pairs have ca. one half the solvent-buried hydrophobic surface area of G-quartets, and ions exert Hofmeister effects by interactions with the surface of biopolymers.^[21] Similarly, G-quartets coordinate dehydrated ions, and high-salt solutions influence biopolymer folding by osmotic effects.^[21,22] We thus reasoned that a DNA duplex and G-quadruplex would exhibit differential destabilization by chaotropes. Here, we demonstrate that perchlorate is a selective denaturant for duplex vs. quadruplex DNA. We have exploited this phenomenon to develop a minimal electron transfer catalyst made of DNA that can be switched between three states: a duplex, a G-quadruplex, and a single-stranded state. We show that this switching can be performed thermally, by dilution, or by concentration. We show that the DNA structure can be switched over 100 times without degradation, and that it can perform multiple-turnover electron transfer catalysis by binding

[a] T. G. Hoog,⁺ M. R. Pawlak,⁺ L. M. Aufdembrink, B. R. Bachan, K. P. Adamala, A. E. Engelhart

Department of Genetics, Cell Biology and Development

University of Minnesota, 6-160 Jackson Hall

321 Church Street SE, Minneapolis, Minnesota 55455 (USA)

E-mail: enge0213@umn.edu

[b] K. P. Adamala, A. E. Engelhart

Department of Biochemistry

Molecular Biology and Biophysics, University of Minnesota

321 Church Street SE, Minneapolis, Minnesota 55455 (USA)

[c] M. B. Galles

Structural Acoustics Branch, NASA Langley Research Center

Mail Stop 463, Hampton, Virginia 23681 (USA)

[d] N. B. Bense

NASA Glenn Research Center

21000 Brookpark Road, Cleveland, Ohio 44135 (USA)

[†] These authors contributed equally to this work.

[**] A previous version of this manuscript has been deposited on a preprint server (<https://www.biorxiv.org/content/10.1101/784561v3>).

 Supporting information for this article is available on the WWW under <https://doi.org/10.1002/cbic.202200090>

 © 2022 The Authors. ChemBioChem published by Wiley-VCH GmbH. This is an open access article under the terms of the Creative Commons Attribution License, which permits use, distribution and reproduction in any medium, provided the original work is properly cited.

hemin and catalyzing electron transfer in the G-quadruplex state (Figure 1).

Results

We designed two FRET reporter systems, **G4-Dark** and **Duplex-Dark** (Figure 2a and Table 1), to allow readout of their folding

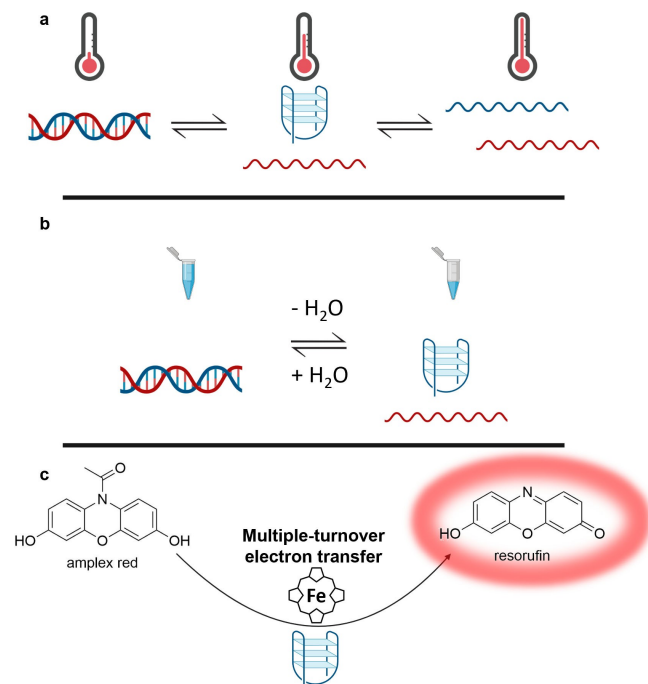


Figure 1. In intermediate perchlorate concentrations, the catalyst can be switched thermally (panel a) through three states. At low temperatures (left), it exists as a duplex; at intermediate temperatures, it exists as a mixture of G-quadruplex and single stranded complement strand (center); and at high temperatures, it is comprised of two single strands (right). At high perchlorate concentrations, it exists in only two states - the G-quadruplex/single stranded complement state (center) and a two-single-strand (right) state. The catalyst can also be switched between two states by varying concentration (panel b). In high-perchlorate solution, the device exists as a G-quadruplex, while in low-perchlorate solution, it forms a duplex. Thus, by diluting a high-salt solution of DNA, the DNA can be switched from a G-quadruplex to a duplex; and by removal of water from a low-salt solution of DNA, the DNA structure can be switched from a duplex to a G-quadruplex. In each case, the G-quadruplex is competent to catalyze multiple-turnover electron transfer in the presence of hemin (panel c and Figure 4).

state. Both reporter systems were of the same length (24 nt) and sequence but differed in fluorophore and quencher placement. **G4-Dark** was comprised of equimolar amounts of **Fluorescein-G4-Quencher**, a DNA sequence that could form a G-quadruplex, and **G4Comp**, its Watson-Crick complement. **Fluorescein-G4-Quencher** was 5'-labeled with a fluorescein tag and 3'-labeled with a quencher. Thus, this system would exhibit fluorescence when **Fluorescein-G4-Quencher** was either unfolded or hybridized to **G4Comp**. When **Fluorescein-G4-Quencher** was folded into a G-quadruplex, fluorophore and quencher would be brought into spatial proximity and quenched.

Duplex-Dark was comprised of equimolar amounts of strands of the same sequences as we employed in **G4-Dark** with rearranged reporters. **Fluorescein-G4**, a 5'-fluorophore-labeled sequence that could form a G-quadruplex, and **G4Comp-Quencher**, a 3' quencher-labeled sequence. In this system, the fluorescein reporter exhibits fluorescence when **Fluorescein-G4** is either folded into a G-quadruplex or is unfolded. Upon hybridization of the two strands to form a double helix, this system would quench.

These strands followed the Hofmeister trend of stability (sulfate > chloride > nitrate > perchlorate). (Supporting Information Figure S1). Both G-quadruplex and duplex structures were increasingly destabilized as chaotropicity of the salts increased; however, duplex was much more susceptible than the G-quadruplex, particularly in sodium perchlorate.

We next examined the thermal response of the **Duplex-Dark** system in LiClO₄ solution (conditions in which only duplex and unfolded states are possible, due to the stability trend in G-quadruplexes (K⁺ > Na⁺ ≫ Li⁺)^[22] (Table 2, Figure 2b, Supporting Information Figures S2–7).^[22] At 100 mM LiClO₄, **Duplex-Dark** exhibited fluorescence response consistent with a double-stranded to unfolded structural transition at 79.8 °C (**Duplex-Dark** possesses spatially adjacent reporters in the duplex state, resulting in a systematic slight elevation of T_M relative to other sequence-related systems with differing tags). As the salt concentration was increased, the thermal midpoint initially increased to a maximum of 84.7 °C in 0.5 M LiClO₄, above which it decreased to a minimum of 50.1 °C in 4 M LiClO₄. This is consistent with electrostatic stabilization effects being predominant at lower salt concentrations and Hofmeister ion effects at higher concentration, as has been previously observed.^[23]

Table 1. Sequences employed in this study.

System/strand	Sequence	Length
G4-Dark		
Fluorescein-G4-Quencher	5'-6-FAM-TG GGT TAG GGA ATT CGG GTT AGG G-lowa Black FQ-3'	24 nt
G4Comp	5'-CCC TAA CCC GAA TTC CCT AAC CCA-3'	24 nt
Duplex-Dark		
Fluorescein-G4	5'-6-FAM-TG GGT TAG GGA ATT CGG GTT AGG G-3'	24 nt
G4Comp-Quencher	5'-CCC TAA CCC GAA TTC CCT AAC CCA-lowa Black FQ-3'	24 nt
G4-SwitchR		
G4Redox	5'-GGG TAG GGC GGG TTG GGA-3'	18 nt
G4Redox-Comp	5'-TCC CAA CCC GCC CTA CCC-3'	18 nt

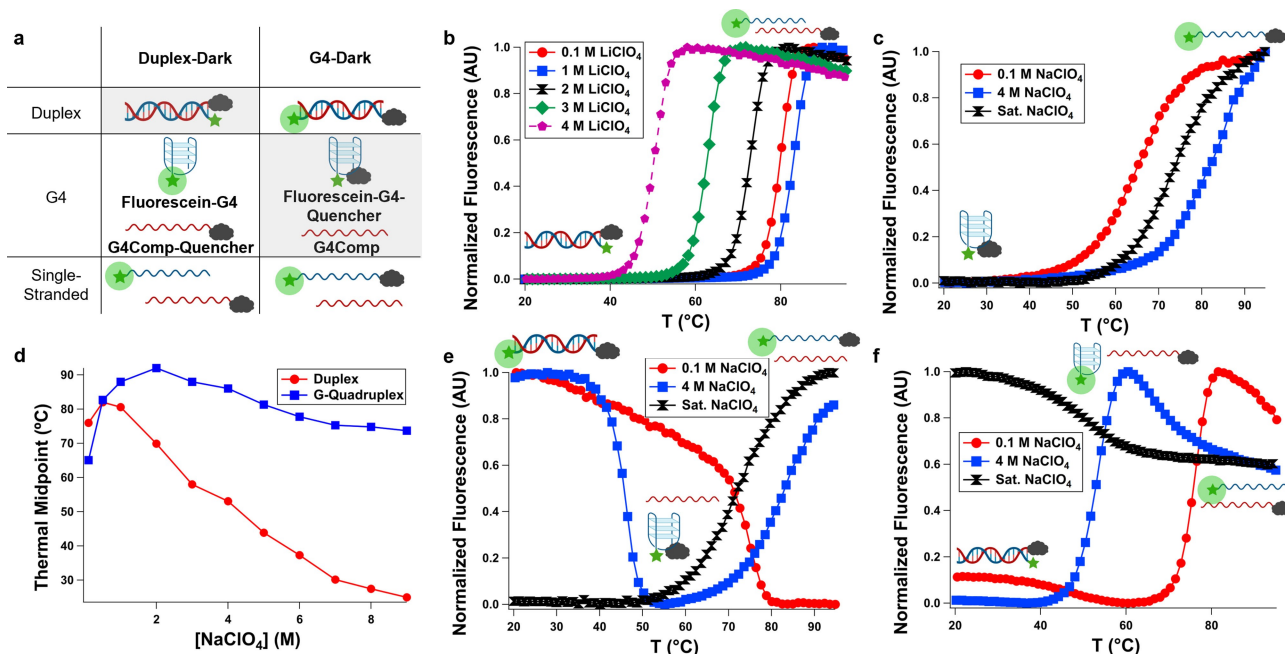


Figure 2. Systems employed in fluorescence-monitored thermal denaturation experiments (panel a). **Duplex-Dark** (left column of panel a) consists of a 5'-fluorescein labeled strand (green star) and a 3'-Iowa Black FQ (grey cloud) strand and can exist in three states: A quenched duplex, a denatured G-quadruplex and single strand, and a denatured set of two single strands. **G4-Dark** (right column of panel a) consists of a dual-labeled (5'-fluorescein, 3'-Iowa Black FQ) strand and its complement and can also exist in three states: A denatured duplex, a quenched G-quadruplex and single strand, and a denatured set of two single strands. When **Duplex-Dark** is operated in LiClO_4 solution, only duplex and single-stranded states are accessible. This transition is destabilized with increasing perchlorate (panel b). When only the **Fluorescein-G4-Quencher** component of **G4-Dark** is operated in NaClO_4 solution (panel c), the G-quadruplex-forming strand is significantly less destabilized by perchlorate (panel d), in contrast to the duplex, which exhibits ca. linear destabilization with increasing NaClO_4 concentration above 1 M (panel d). As a result of this differential stability, **G4-Dark** (panel e) and **Duplex-Dark** (panel f) can be switched thermally between duplex, G-quadruplex, and single-stranded states, and the temperatures at which these transitions occur can be tuned by varying the concentration of NaClO_4 . In low perchlorate (0.1 M), only the duplex-to-single stranded transition is observed (red circles). In intermediate perchlorate (4 M), the DNA structure transitions between duplex (at low temperature), G-quadruplex (at intermediate temperature), and single-stranded (at high temperature) states (blue squares). In high perchlorate (saturated, ca. 9.5 M), the DNA structure exists only in the G-quadruplex and single-stranded states (black hourglasses).

Table 2. Thermal midpoints ($^{\circ}\text{C}$) of **G4-Dark**, **Duplex-Dark**, and **Fluorescein-G4-Quencher** in NaClO_4 solution, and of **G4-Dark** and **Duplex-Dark** in LiClO_4 solution.

Strands/ $[\text{ClO}_4^-]$ (M)		0.1	0.5	1	2	3	4	5	6	7	8	Sat.
Duplex-Dark (Fluorescein-G4 and G4Comp-Quencher)/ LiClO_4 ^[c]	G4	none	none	none	none	none	none	n/d ^[d]				
	duplex	79.8	84.7	83.0	72.7	62.6	50.1					
Fluorescein-G4-Quencher/NaClO₄	G4	65.1	82.7	88 ^[a]	92 ^[a]	88 ^[a]	86 ^[a]	81.3	77.8	75.1	74.9	73.7
	duplex	n/a	n/a	n/a	n/a	n/a	n/a	n/a	n/a	n/a	n/a	n/a
G4-Dark (Fluorescein-G4-Quencher and G4Comp)/ NaClO_4	G4	none	none	high ^[a]	high ^[a]	83.2	83.0	80.2	78.1	75.3	74.4	72.6
	duplex	73.9	77.4	73.8	66.7	48.8	45.6	37.0	32.2	27.0	low ^[b]	low ^[b]
Duplex-Dark (Fluorescein-G4 and G4Comp-Quencher)/ NaClO_4	G4	n/a	n/a	n/a	n/a	n/a	n/a	n/a	n/a	n/a	n/a	n/a
	duplex	75.9	82.0	80.5	69.9	58.2	53.1	43.9	37.3	30.3	27.6	low ^[b]
G4-Dark (Fluorescein-G4-Quencher and G4Comp)/ LiClO_4 ^[c]	G4	none	none	none	none	none	none	n/d ^[d]				
	duplex	76.6	81.5	80.2	69.9	57.7	46.6					

[a] Unfolding transition not complete at 95°C so sigmoid fit not possible, number reported obtained using first derivative method where possible. [b] Folding transition not complete at 20°C . [c] Only duplex-single stranded transition is observed in this system due to the absence of sodium and reporters used. [d] Not determined owing to the lower solubility of LiClO_4 vs. NaClO_4 .

We next examined the thermal response of the **Fluorescein-G4-Quencher** component of **G4-Dark** in NaClO_4 -containing solution to ascertain the impact of this salt on the stability of the G-quadruplex states of this system (Figure 2c, Supporting Information Figures S8–18). In all NaClO_4 -containing solutions, **Fluorescein-G4-Quencher** formed a G-quadruplex, giving a 65.1°C thermal midpoint in 100 mM NaClO_4 ; this temperature

increased with increasing NaClO_4 , consistent with the electrostatic screening afforded by Na^+ as well as its binding to the central channel within the G-quadruplex. Between 1–4 M NaClO_4 , the G-quadruplex was so stable it was not fully denatured, even at 95°C (representative melting curve of 4 M NaClO_4 in Figure 2c). In 5 M NaClO_4 and above, thermal midpoints were measurable and decreased with increasing

perchlorate but remained high. Even in saturated NaClO_4 (ca. 9.5 M and containing less than three water molecules per ion), **Fluorescein-G4-Quencher** exhibited a higher thermal midpoint (73.7 °C) than in 100 mM NaClO_4 (65.1 °C).

The destabilization of the DNA duplex in **G4-Dark** and **Duplex-Dark** was marked (Figure 2d) and exhibited a near-linear response in thermal midpoint of $-7^\circ\text{C}/\text{M}$ NaClO_4 between 1 and 9 M ($r^2=0.97$); these duplexes exhibited thermal midpoints of ca. 75 °C at 100 mM NaClO_4 and ca. 27–30 °C at 7–8 M NaClO_4 . In contrast, perchlorate-induced destabilization of the G-quadruplex formed by the G-rich strands was less pronounced and/or more than compensated by the presence of additional sodium (Figure 2d). **Fluorescein-G4-Quencher** exhibited a thermal midpoint of 65.1 °C at 100 mM NaClO_4 and 73.7 °C in saturated sodium perchlorate (ca. 9.5 M). That is, in a polymorphic sequence, one possible secondary structure (dsDNA) that is *more* stable in low perchlorate than an alternative fold (a G-quadruplex) becomes *less* stable than the alternative fold in high perchlorate.

Because of this, we speculated that **G4-Dark** could be thermally switched between all three states (duplex, G-quadruplex, and single-stranded) at intermediate perchlorate concentrations. (Figure 2e, Supporting Information Figures S19–29). Consistent with this, we observed a single transition at low (0.1 M) NaClO_4 , which corresponded to the duplex-to-single-strand transition. At high NaClO_4 (saturated/ca. 9.5 M), we also observed a single transition, which corresponded to the G-quadruplex to single-strand transition (Figure 2e), confirmed by the lack of thermal dequenching under these conditions with **Duplex-Dark** (Figure 2f).

We next sought to characterize the reversibility of cycling through the DNA structural states. Reversibility without degradation is essential to a switchable catalyst and a potential concern given some structure-switching nanodevices' propensity to exhibit degradation with repeated switching due to buildup of waste products.^[16,18] To do so, we thermally cycled a sample of **G4-Dark** in 4 M NaClO_4 (conditions in which all three states are thermally accessible) 100 times while monitoring fluorescence. The sample did not exhibit degradation during this experiment (Figure 3a–d).

Given the results from Figure 2, we reasoned that it would be possible to switch the state of our catalyst from G-quadruplex to duplex (by diluting it with aqueous buffer, lowering the concentration of perchlorate) or from duplex to G-quadruplex (by removing water under vacuum, increasing the concentration of perchlorate). To do so, we performed dilutions of high-salt solutions of **G4-Dark** (which would initially exist in its dark state and transition to its light state) and **Duplex-Dark** (which would initially exist in its light state and transition to its dark state). **G4-Dark** recovered fluorescence upon dilution from 8 M to 0.8 M, and **Duplex-Dark** lost fluorescence following the same dilution (Figure 3e). Conversely, we sought to switch the system by removal of solvent. To do so, we took samples with an initial volume of 200 μL and initial concentration of 0.8 M NaClO_4 and placed them in a vacuum chamber. We monitored these samples by fluorescence imaging with a custom-built device (Supporting Information Figures S30–37). The samples,

initially in low NaClO_4 , behaved as expected for the duplex state, with **G4-Dark** exhibiting fluorescence and **Duplex-Dark** in a dark state. **Duplex-Dark** remained dark during concentration while the fluorescence of **G4-Dark** gradually increased as the solution became more concentrated. Finally, both solutions reached a critical concentration of NaClO_4 at which they transitioned to the G-quadruplex state: **Duplex-Dark** became fluorescent and **G4-Dark** became nonfluorescent (Figure 3f–i, Supporting Information Videos S1 and 2, Supporting Information Code S1–3). Increases in strand concentration, as would be expected to occur concomitantly with concentration of salt, impacted the bimolecular duplex stability only slightly (Supporting Information Table S1).

G4-Dark and **Duplex-Dark** demonstrate the perchlorate-based switchability of our system. To demonstrate the ability of G-quadruplex/duplex equilibria to enable switchable electron transfer, we constructed **G4-SwitchR** (switchable redox; Table 1), which was comprised of **G4Redox** (a sequence previously shown to form a highly active peroxidase in complex with hemin),^[24] **G4Redox-Comp**, and the cofactor hemin. This G-quadruplex was shorter (18 nt) than the FRET systems used, but it behaved similarly in perchlorate solutions. We employed Amplex Red, a nonfluorescent dye that is oxidized to the fluorescent, red-colored pigment resorufin catalytically by the peroxidase-mimicking DNAzyme formed between a G-quadruplex and hemin (Figure 4a–c).^[25]

We compared the ratio of the rate of electron transfer performed by the G-quadruplex/hemin complex to that performed by hemin alone (Figure 4d). In 0.1 and 5 M NaClO_4 , the **G4Redox** component of **G4-SwitchR** binds hemin and can perform electron transfer, with enhanced activity in 5 M relative to 0.1 M NaClO_4 (Figure 4e, Supporting Information Table S2, Supporting Information Figures S38). In saturated NaClO_4 , electron transfer is suppressed due to lack of hemin-G-quadruplex interactions.

In 0.1 M NaClO_4 , **G4-SwitchR** exists entirely as a duplex, hemin binding is thus abrogated (Supporting Information Figure S39); resorufin was produced at <30 nM/min when **G4-SwitchR** was present or when it was absent (Figure 4f). In 5 M NaClO_4 , **G4-SwitchR** dissociates into **G4Redox** folded into a G-quadruplex, which is competent to bind hemin (Supporting Information Figure S40), and **G4Redox-Comp** exists as a single strand. The resulting hemin-**G4Redox** complex performs electron transfer (as measured by the reporter dye Amplex Red's conversion to resorufin) 35-fold more rapidly than hemin alone (Supporting Information Figure S38): the hemin-**G4Redox** complex produced resorufin at 300 nM/min vs. unbound hemin, which produced it at 9 nM/min. At still higher NaClO_4 , hemin-G-quadruplex binding decreases (as indicated by a decreased Soret peak, Supporting Information Figure S39), and in saturated (ca. 9.5 M) NaClO_4 , resorufin was produced at a much lower rate of 46 nM/min. Hemin remained in solution at this concentration of NaClO_4 (Supporting Information Figure S41). Consistent with the propensity of hemin to aggregate,^[26] partial loss of hemin was observed on extended centrifugation. However, this occurred in both low- and high-perchlorate solutions, indicating this is not a perchlorate-induced phenom-

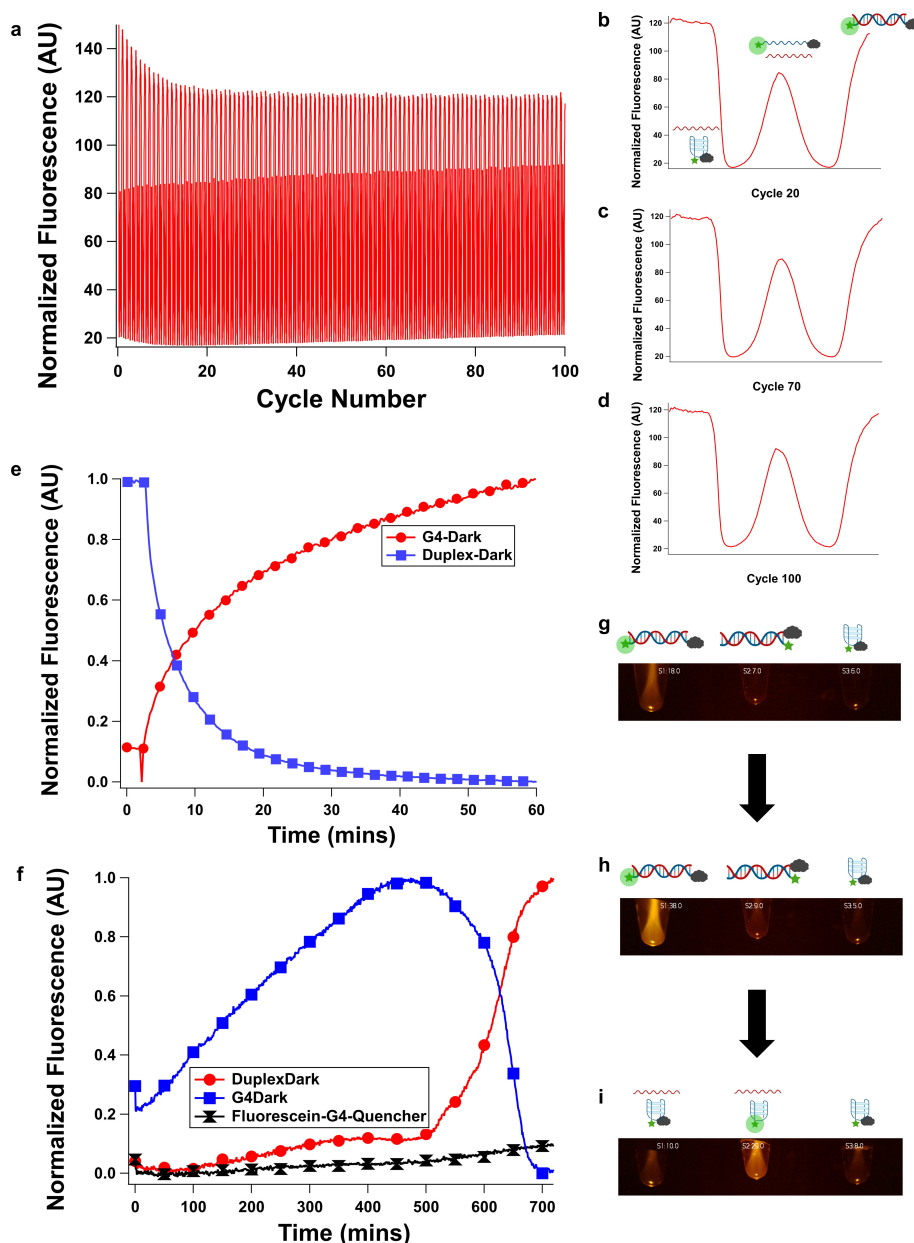


Figure 3. Switching behavior of G4-Dark. G4-Dark (which reports on all three states) was switched thermally 100 times between duplex, G-quadruplex, and single-stranded states with no decay of fluorescence signal following an initial 10-cycle “burn-in” (panel a shows the full series of switching events; panels b-d show cycles 20, 70 and 100). While thermal switching is rapid, a “latching” behavior with slower switching is possible with chemical switching, enabling a high level of temporal control of DNA structure switching. To demonstrate this, G4-Dark and Duplex-Dark were also switched chemically by dilution on slower timescales, enabling refolding from the G-quadruplex to duplex state (panel e) and vacuum concentration, enabling refolding from the duplex to G-quadruplex state. In vacuum experiments, G4-Dark (left) Duplex-Dark (center) and Fluorescein-G4-Quencher (right) were employed (panel f shows fluorescence quantitated from images, panels g-i show various timepoints, and this experiment is shown in Supporting Information Videos S1 and 2). Under all conditions, Fluorescein-G4-Quencher remained a G-quadruplex and did not emit fluorescence. At low (0.8 M) NaClO_4 , the duplex state was favored, resulting in G4-Dark emitting fluorescence and Duplex-Dark existing in a fluorescence-quenched state (panel g). At intermediate perchlorate concentrations during vacuum concentration, the fluorescence of G4-Dark increased due to an increase in oligonucleotide concentration but an insufficient increase in NaClO_4 concentration to induce a structure change; G4-Dark remained fluorescent and Duplex-Dark remained in a quenched state due to this (panel h). Finally, upon ca. 10-fold concentration (to ca. 8 M NaClO_4 , meniscus demonstrating ca. 10-fold concentration from 200 to 20 μL visible) G4-Dark and Duplex-Dark assumed their G-quadruplex states, causing G4-Dark to quench and Duplex-Dark to become fluorescent (panel i). Brightness was increased by 50% in panels g-i relative to captured images for visual clarity. Original images with plots of image-quantitated fluorescence and annotations are shown in Supporting Information Videos S1 and 2.

enon. G-quadruplex-dependent Soret absorbance for hemin was observed (Supporting Information Figure S39), demonstrating G-quadruplex/hemin interactions. Additionally, heme

dimers exhibit extremely low electron transfer catalysis behavior, consistent with G-quadruplex hemin being the active species.^[27] Thus, perchlorate concentration can be varied to

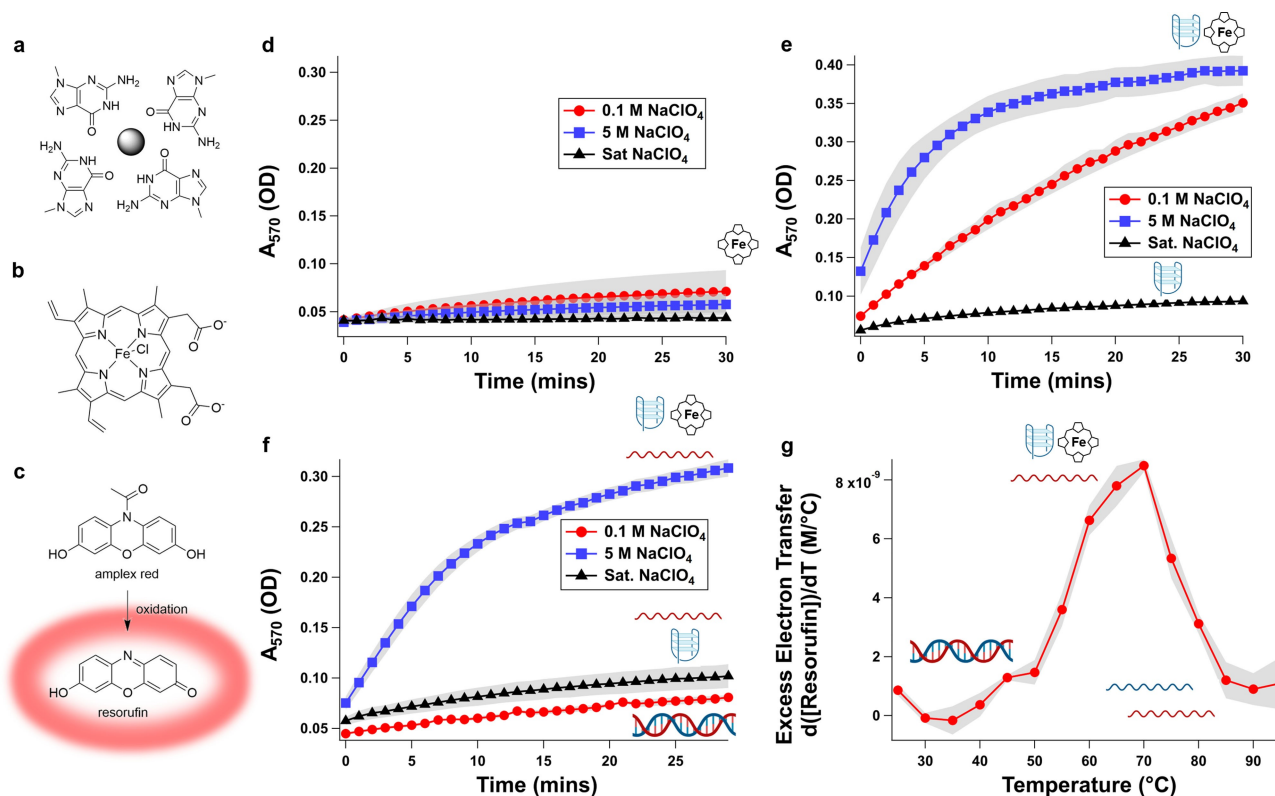


Figure 4. Switchable electron transfer amplification behavior of **G4-SwitchR**-hemin complex. When folded into the G-quadruplex state, a solvent-exposed G-quartet (panel a) is present which is known to provide a tight binding pocket for the cofactor hemin (panel b); the complex formed by a G-quadruplex and hemin can catalyze electron transfer. We visualize this here using the colorimetric electron transfer probe Amplex Red (panel c, top), which is initially colorless and nonfluorescent and, when oxidized, converts to the red fluorescent pigment resorufin (panel c, bottom). Hemin itself has a minimal background rate of electron transfer that is suppressed by increasing NaClO_4 concentration (panel d). When **G4-Redox** is operated as the only oligonucleotide constituent (i.e., under conditions in which the strand will form only a G-quadruplex) in the presence of hemin, robust multiple-turnover electron transfer occurs in low (0.1 M, red circles) NaClO_4 solution, it is enhanced in moderate (5 M, blue squares) NaClO_4 solution, and it is suppressed in saturated NaClO_4 solution (black triangles) due to abrogation of hemin binding (panel e). When **G4-SwitchR** is operated in these same conditions, electron transfer is switched off in low (0.1 M) NaClO_4 solution due to duplex formation, switched on in moderate (5 M) NaClO_4 solution due to G-quadruplex formation with concomitant hemin binding, and switched off in saturated NaClO_4 solution due to abrogation of hemin binding (panel f). **G4-SwitchR** can also be switched thermally, exhibiting varying rate of reaction depending on its folding state. When ramped from 25 to 95 °C in 5 M NaClO_4 solution, excess electron transfer (as measured by rate of resorufin production in excess of that observed in hemin alone) starts at near-zero as the DNA structure exists in duplex form, increases substantially between 50 and 70 °C as the duplex melts and the G-quadruplex forms, and it decreases again by ca. 90% between 70 and 90 °C as the G-quadruplex unfolds and the single-stranded form of the DNA system forms (panel g). These results are consistent with UV-visible monitored thermal measurements of secondary structures formed (Supporting Information Figures S43-44). Error bar shading = S.E.M., $n = 3$ technical replicates.

switch the state of the active G-quadruplex/hemin form of the catalyst, as well as to modulate the reaction rate.

In addition to Amplex Red, we tested **G4-SwitchR** with the peroxidase substrates 3,3',5,5'-Tetramethylbenzidine (TMB) and 2,2'-azino-bis(3-ethylbenzothiazoline-6-sulfonic acid) (ABTS), and observed that these dyes acted as electron donors in this system, demonstrating the diversity of substrates that can be oxidized in this system (Supporting Information Figure S42).

In order to demonstrate that thermally switching DNA conformation could also switch electron transfer catalysis, we measured Amplex Red oxidation using **G4-SwitchR** in 4 M NaClO_4 (Figure 4g). At 20 °C, electron transfer was near-zero. As the sample was heated and switched from duplex to G-quadruplex, the rate of electron transfer exhibited a significant increase, reaching a maximum at 60 °C and again decreasing as the G-quadruplex unfolded. This is consistent with the thermal

denaturation curve generated by monitoring A_{295} (a diagnostic wavelength for G-quadruplex formation) of **G4-SwitchR** (Supporting Information Table S2, Supporting Information Figures S43-44). Notably, hydrogen peroxide was required. Perchlorate ion, despite its exceptionally high oxidation potential, did *not* suffice as an electron acceptor in this system.

Discussion

Here, we have demonstrated that duplex DNA is preferentially destabilized by perchlorate salts relative to G-quadruplex DNA, and that this enables solution conditions-selective formation of DNA-hemin complexes that can act as electron transfer catalysts. This phenomenon can be used to switch electron transfer behavior in three ways: 1) direct addition of perchlorate

salts, 2) thermal switching, and 3) increasing perchlorate salt concentration by vacuum concentration.

While the results here relate to switching of secondary structure in high-salt solution, examples of secondary-structure remodeling are observed in life as well. Nucleic acids exhibit considerable polymorphism in biological systems, particularly in sequences that can form G-quadruplexes. Such systems are diverse and widespread in biology and extend to both DNA and RNA, including proto-oncogene promoters,^[33] the expansion segments of rRNA of higher organisms,^[34–36] the rDNA corresponding to those expansion segments,^[37] and eukaryotic messenger RNAs.^[12,13] Several proteins can remodel G-quadruplexes, and both energy-dependent (i.e., helicases) and energy-independent systems that can do so have been reported.^[38,39] ATP-dependent helicases are known to unwind G-quadruplex structures, and the RNA-binding protein Lin28 has been shown to unfold G-quadruplexes without the requirement for ATP.^[38]

Given that such remodeling processes are also operative in nature and that hemin-G-quadruplex promoted electron transfer has been suggested as being physiologically relevant, we speculate that conditional hemin-G-quadruplex complexes are a means by which cells could conditionally enable electron transfer.^[40] For example, ribosomes from the neurons of Alzheimer's Disease patients have been shown to contain more iron than those from healthy patients, and these ribosomes possess peroxidase activity.^[41] G-quadruplexes may enable this phenomenon *in vivo*. Human ribosomes are known to be polymorphic, particularly in their G-rich expansion segments, some of which have been observed to lack electron density in EM maps, consistent with an equilibrium between multiple states.^[34,42] Rarely, individual ribosomes clearly exhibit extended conformations consistent with Watson-Crick base pairing, but these same sequences possess exceptionally high G-quadruplex forming potential and form G-quadruplexes in cell-free *in vitro* experiments, which is consistent with polymorphism with one state capable of catalyzing electron transfer.^[36,37]

Beyond the high-salt solutions that are the focus of the present study, we suggest that conditionally folded G-quadruplexes in cells could collaborate with hemin, producing a means by which cells can perform conditional electron transfer that is analogous to the phenomenon we have employed in this work. In fact, recent work suggests that hemin-G-quadruplex associations occur in human cells.^[40] Such a phenomenon could be exploited both by extant life or in synthetic biological systems, and we speculate this could have enabled conditionally active forms of prebiotic electron transfer catalysts, which have attracted intense interest in recent years.^[6,43,44]

Experimental Section

Nucleic acids: Oligonucleotides were obtained from Integrated DNA Technologies (Coralville, IA) and used as received. Labeled strands were obtained with HPLC purification and unlabeled strands were obtained with standard desalting.

DNA sample preparation: Oligonucleotides were annealed in a T100 thermal cycler (Bio-Rad) by incubating at 95 °C for 2 minutes, then decreasing the temperature by 10 °C steps and annealing at each step for 1 minute to a final temperature of 25 °C. Except where otherwise specified, experiments were performed in 50 mM Li-HEPES, pH 7.4, with 1 μM of the duplexed or single stranded oligonucleotides.

Fluorescence-monitored experiments: Fluorescence measurements were performed using a Gemini XS plate reader (Molecular Devices) or a Cary Eclipse (Varian Technologies) fluorometer equipped with a thermostated peltier holder (Agilent Technologies) when bidirectional temperature control was required. Excitation was performed at 495 nm and emission was monitored at 520 nm.

For thermal denaturation studies, the sample was ramped from 20 °C to 95 °C (two heat/cool cycles) at 5 °C/min. Selected measurements were also performed with a slower 0.5 °C/min ramp rate to mitigate hysteresis. Thermal midpoints are reported as a sigmoid fit of the transition(s) in the second heating trace of two temperature ramps.

Data from fluorescence melts were normalized by division, setting the highest RFU value to 1 and the lowest value to 0 for each state in a given system (quenched or dequenched/partially dequenched).

UV-Vis monitored experiments: Thermal denaturation experiments were performed using a qCHANGER 6/Cary60 (Quantum Northwest) interfaced to a Cary 60 UV-Visible spectrophotometer (Agilent Technologies) using a custom ADL script developed by Quantum Northwest to collect full spectra at each temperature as described previously. Heat sinking for the Peltier device was provided by an EXT-440CU ambient liquid cooling system (Koolance). Duplex melting transitions were monitored using the 260 nm trace from these datasets and G-quadruplex melting temperatures were monitored using the 295 nm trace.

Amplex Red experiments (described further below) were monitored on a Cary 60 UV-vis (Agilent Technologies) or a SpectraMAX 340PC plate reader (Molecular Devices) with the PathCheck functionality enabled.

Circular dichroism (CD) experiments: CD spectra were obtained using a JASCO J-815 Circular Dichroism Spectropolarimeter and an attached 6-sample Peltier Turret Cell Changer (Model MPTC-490S/15). Spectra were obtained at 25 °C from 220–350 nm with 1 nm increments and averaged over three scans. The solutions consisted of 5 mM phosphate buffer pH 7.4, 20 μM oligonucleotide, 20 μM hemin, 2% DMSO (from hemin stock). **G4SwitchR-Comp** signal was subtracted from the **G4SwitchR** spectra.

Fluorescence imaging under vacuum: Samples were pipetted into PCR tubes with the lids open, which were inserted into a 3D-printed jig that was placed inside a black box. The jig was fabricated in PLA on a Prusa 3D printer. The box and its contents were placed in a vacuum desiccator (Supporting Information Figures S29–36) and the chamber was continuously evacuated with a diaphragm pump (Welch 2014B-01). The samples were excited with LEDs with emission centered at 462–465 nm (Item B01GDO9UNY, Amazon). The samples were imaged with a camera (Raspberry Pi Module V2, Amazon) fixed at 90° relative to the light sources. A 12.5 mm longpass filter (Schott OG 550, Edmund Optics) was affixed with polyvinyl acetate adhesive (Elmer's Glue-All, Costco Wholesale) directly in front of the camera lens to block excitation light and pass emitted light. The camera was interfaced to a Raspberry Pi B+ (Amazon). A Python script controlled the Raspberry Pi's GPIO pins to illuminate samples at 1-minute intervals, collect images, and measured and

plotted fluorescence intensity vs. time. Time-lapse movies were generated from captured images using FFmpeg.

Samples were prepared with a starting volume of 200 μL and 0.1 μM of **G4-Dark**, **Duplex-Dark**, or **Fluorescein-G4-Quencher** in 5 mM Li-HEPES, pH 7.4 and 0.8 M NaClO_4 . After desiccation, the final volume was 20 μL with 50 mM Li-HEPES, 8 M NaClO_4 and 1 μM **G4-Dark**, **Duplex-Dark**, or **Fluorescein-G4-Quencher**.

Electron transfer assay: Samples contained **G4-SwitchR** (i.e., **G4Redox** and **G4Redox-Comp**), **G4Redox** alone, or no oligonucleotide. **G4Redox**, when present, was at 5 μM and **G4Comp**, when present, was at 10 μM to ensure full duplex state at low perchlorate/temperature and that electron transfer catalysis observed was due to the G-quadruplex state of **G4-SwitchR** and not residual unduplexed **G4Redox**. The buffer used here was 5 mM sodium phosphate, pH 7.4 with varying sodium perchlorate concentrations. To initiate the reaction, hemin was added to a final concentration of 1 μM , hydrogen peroxide was added to a final concentration of 300 μM , and Amplex Red was added to a final concentration of 200 μM . Reactions were monitored by measuring the absorbance of resorufin at 570 nm. For the Cary 60 thermal activation-Amplex red assay, Amplex Red was added to a final concentration of 2 mM. All reactions contained 2% DMSO, which came from the hemin and Amplex Red stocks.

Similar reaction conditions were used for TMB and ABTS assays with the following exceptions. TMB: 50 mM Li-HEPES pH 7.4, 2 mM TMB, 1 mM hydrogen peroxide, 10% DMSO. ABTS: 10 mM MES buffer pH 5.1, 1 mM ABTS, 1 mM hydrogen peroxide, 10% DMSO.

Precipitation assay: Solutions consisted of 5 μM **G4Redox** and 1 μM hemin in 5 mM phosphate buffer pH 7.4 and 2% DMSO with varying sodium perchlorate. UV-vis spectra were obtained from 230–500 nm at 0 minutes and 60 minutes. After 60 minutes, the samples were centrifuged at 13,000 rpm for 10 minutes and 200 μL of supernatant was used to collect a spectrum.

Code Availability Statement

All computer code used during the current study is included in this published article (and its Supporting Information files).

Acknowledgements

Several figures in this manuscript were prepared using BioRender.com. We thank Loren Williams and George Perry for helpful discussions. The imaging apparatus used here was developed as part of the RockSat-C 2018 sounding rocket program, sponsored by the Colorado Space Grant Consortium and NASA Wallops; we thank the NASA PAXC team members for helpful discussions. This work was supported by NASA Contract 80NSSC18K1139 under the Center for Origin of Life (to A.E.E. and K.P.A.).

Conflict of Interest

The authors declare no competing interests.

Data Availability Statement

The datasets generated during and/or analyzed during the current study are available from the corresponding author on reasonable request.

Keywords: DNA · chaotropes · nanotechnology · electron transfer · synthetic biology

- [1] G. Reguera, K. D. McCarthy, T. Mehta, J. S. Nicoll, M. T. Tuominen, D. R. Lovley, *Nature* **2005**, *435*, 1098–1101.
- [2] Y. Wang, Z. Tang, S. Tan, N. A. Kotov, *Nano Lett.* **2005**, *5*, 243–248.
- [3] S. Vecchioni, M. C. Capece, E. Toomey, L. Nguyen, A. Ray, A. Greenberg, K. Fujishima, J. Urbina, I. G. Paulino-Lima, V. Pinheiro, J. Shih, G. Wessel, S. J. Wind, L. Rothschild, *Sci. Rep.* **2019**, *9*, 6942.
- [4] T. Nishinaka, A. Takano, Y. Doi, M. Hashimoto, A. Nakamura, Y. Matsushita, J. Kumaki, E. Yashima, *J. Am. Chem. Soc.* **2005**, *127*, 8120–8125.
- [5] B. Wildt, P. Mali, P. C. Searson, *Langmuir* **2006**, *22*, 10528–10534.
- [6] J. D. Kim, D. H. Pike, A. M. Tyryshkin, G. V. T. Swapna, H. Raanan, G. T. Montelione, V. Nanda, P. G. Falkowski, *J. Am. Chem. Soc.* **2018**, *140*, 11210–11213.
- [7] D. Sen, L. C. H. Poon, *Crit. Rev. Biochem. Mol. Biol.* **2011**, *46*, 478–492.
- [8] E. Raven, B. Dunford, Eds., *Heme Peroxidases*, Royal Society Of Chemistry, Cambridge, **2015**.
- [9] P. Travascio, Y. Li, D. Sen, *Chem. Biol.* **1998**, *5*, 505–517.
- [10] E. Golub, R. Freeman, I. Willner, *Angew. Chem. Int. Ed.* **2011**, *50*, 11710–11714; *Angew. Chem.* **2011**, *123*, 11914–11918.
- [11] J. H. Dawson, *Science* **1988**, *240*, 433–439.
- [12] J. U. Guo, D. P. Bartel, *Science* **2016**, *353*, aaf5371.
- [13] S. Y. Yang, P. Lejault, S. Chevrier, R. Boidot, A. G. Robertson, J. M. Y. Wong, D. Monchaud, *Nat. Commun.* **2018**, *9*, 4730.
- [14] M. C. Chen, R. Tippiana, N. A. Demeshkina, P. Murat, S. Balasubramanian, S. Myong, A. R. Ferré-D'Amaré, *Nature* **2018**, *558*, 465–469.
- [15] B. Yurke, A. J. Turberfield, A. P. Mills, Jr., F. C. Simmel, J. L. Neumann, *Nature* **2000**, *406*, 605–608.
- [16] P. Alberti, J.-L. Mergny, *Proc. Natl. Acad. Sci. USA* **2003**, *100*, 1569–1573.
- [17] D. Liu, S. Balasubramanian, *Angew. Chem. Int. Ed.* **2003**, *42*, 5734–5736; *Angew. Chem.* **2003**, *115*, 5912–5914.
- [18] J. D. Bishop, E. Klavins, *Nano Lett.* **2007**, *7*, 2574–2577.
- [19] C. Wang, Z. Huang, Y. Lin, J. Ren, X. Qu, *Adv. Mater.* **2010**, *22*, 2792–2798.
- [20] C. Shao, N. Lu, D. Sun, *Chin. J. Chem.* **2012**, *30*, 1575–1581.
- [21] L. M. Pegram, T. Wendorff, R. Erdmann, I. Shkel, D. Bellissimo, D. J. Felitsky, M. T. Record, Jr., *Proc. Natl. Acad. Sci. USA* **2010**, *107*, 7716–7721.
- [22] N. V. Hud, F. W. Smith, F. A. Anet, J. Feigon, *Biochemistry* **1996**, *35*, 15383–15390.
- [23] A. Salis, B. W. Ninham, *Chem. Soc. Rev.* **2014**, *43*, 7358–7377.
- [24] W. Li, Y. Li, Z. Liu, B. Lin, H. Yi, F. Xu, Z. Nie, S. Yao, *Nucleic Acids Res.* **2016**, *44*, 7373–7384.
- [25] M. Zhou, Z. Diwu, N. Panchuk-Voloshina, R. P. Haugland, *Anal. Biochem.* **1997**, *253*, 162–168.
- [26] W. I. White, in *The Porphyrins*, Elsevier, **1978**, pp. 303–339.
- [27] S. B. Brown, T. C. Dean, P. Jones, *Biochem. J.* **1970**, *117*, 741–744.
- [28] M. H. Lee, S. J. Kim, D. Chang, J. Kim, S. Moon, K. Oh, K.-Y. Park, W. M. Seong, H. Park, G. Kwon, B. Lee, K. Kang, *Mater. Today* **2019**, *29*, 26–36.
- [29] **N.d.**
- [30] E. Golub, R. Freeman, I. Willner, *Anal. Chem.* **2013**, *85*, 12126–12133.
- [31] O. J. Einarson, D. Sen, *Nucleic Acids Res.* **2017**, *45*, 9813–9822.
- [32] C. Wang, G. Jia, J. Zhou, Y. Li, Y. Liu, S. Lu, C. Li, *Angew. Chem. Int. Ed.* **2012**, *51*, 9352–9355; *Angew. Chem.* **2012**, *124*, 9486–9489.
- [33] S. Balasubramanian, L. H. Hurley, S. Neidle, *Nat. Rev. Drug Discovery* **2011**, *10*, 261–275.
- [34] H. Khatler, A. G. Myasnikov, S. K. Natchiar, B. P. Klaholz, *Nature* **2015**, *520*, 640–645.
- [35] S. K. Natchiar, A. G. Myasnikov, H. Kratzat, I. Hazemann, B. P. Klaholz, *Nature* **2017**, *551*, 472–477.
- [36] S. Mestre-Fos, P. I. Penev, S. Suttapitugsakul, M. Hu, C. Ito, A. S. Petrov, R. M. Wartell, R. Wu, L. D. Williams, *J. Mol. Biol.* **2019**, *431*, 1940–1955.

- [37] D. Drygin, J. Whitten, W. Rice, S. O'Brien, M. Schwaebe, A. Lin, C. Ho, K. Trent, *Cancer Res.* **2008**, *68*, 3301–3301.
- [38] E. O'Day, M. T. N. Le, S. Imai, S. M. Tan, R. Kirchner, H. Arthanari, O. Hofmann, G. Wagner, J. Lieberman, *J. Biol. Chem.* **2015**, *290*, 17909–17922.
- [39] O. Mendoza, A. Bourdoncle, J.-B. Boulé, R. M. Brosh, Jr., J.-L. Mergny, *Nucleic Acids Res.* **2016**, *44*, 1989–2006.
- [40] L. T. Gray, E. Puig Lombardi, D. Verga, A. Nicolas, M.-P. Teulade-Fichou, A. Londoño-Vallejo, N. Maizels, *Cell Chem. Biol.* **2019**, *26*, 1681–1691.e5.
- [41] K. Honda, M. A. Smith, X. Zhu, D. Baus, W. C. Merrick, A. M. Tartakoff, T. Hattier, P. L. Harris, S. L. Siedlak, H. Fujioka, Q. Liu, P. I. Moreira, F. P. Miller, A. Nunomura, S. Shimohama, G. Perry, *J. Biol. Chem.* **2005**, *280*, 20978–20986.
- [42] A. M. Anger, J.-P. Armache, O. Berninghausen, M. Habeck, M. Subklewe, D. N. Wilson, R. Beckmann, *Nature* **2013**, *497*, 80–85.
- [43] C. Bonfio, E. Godino, M. Corsini, F. Fabrizi de Biani, G. Guella, S. S. Mansy, *Nat. Catal.* **2018**, *1*, 616–623.
- [44] K. B. Muchowska, S. J. Varma, J. Moran, *Nature* **2019**, *569*, 104–107.

Manuscript received: February 11, 2022
Revised manuscript received: March 2, 2022
Accepted manuscript online: March 4, 2022
Version of record online: March 23, 2022